

Optimal Control of Differentially Flat Systems is Surprisingly Simple

Logan E. Beaver, *IEEE Student Member*, Andreas A. Malikopoulos, *IEEE Senior Member*

Abstract—As we move to increasingly complex cyber-physical systems (CPS), new approaches are needed to plan efficient state trajectories in real-time. In this paper, we propose an approach to significantly reduce the complexity of solving optimal control problems for a class of CPS. We exploit the property of differential flatness to simplify the Euler-Lagrange equations, and this simplification eliminates the numerical instabilities that arise in the general case. We also present an explicit differential equation that describes the evolution of the optimal state trajectory, and we extend our results to consider both the unconstrained and constrained cases. Furthermore, we demonstrate the performance of our approach by generating the optimal trajectory for a double-integrator agent in an environment with an obstacle. In simulation, our approach shows a 30% cost reduction and nearly a 3-fold increase in computational speed compared to existing collocation-based optimal control libraries.

I. INTRODUCTION

There is an increasing demand to push the boundaries of autonomy in cyber-physical systems (CPS) using experimental testbeds [1]–[4] and outdoor experiments [5], [6]. As CPS achieve higher autonomy levels, they will be forced into complicated interactions [7] with other agents [8] and the surrounding environment [9]. These autonomous agents must be able to react quickly to their environment and re-plan efficient trajectories. To this end, we propose a new method to simplify real-time optimal trajectory planning by exploiting differential flatness.

A system is differentially flat if there exist a set of endogenous *flat* variables, also called outputs, such that the original state and control variables can be written as an explicit function of the flat variables and a finite number of their derivatives. This yields an equivalent flat system that is completely described by integrator dynamics. Differentially flat systems have garnered significant interest since their introduction [10], and it has been shown that generating trajectories in the flat space can reduce computational time by at least an order of magnitude [11]. Differentially flat systems are closely related to feedback linearizable systems [12]; however, the standard control techniques for flat systems are distinct from feedback linearization.

The overwhelming majority of research on trajectory generation with differential flatness uses collocation techniques, i.e., finding optimal parameters for a set of basis functions in the flat output space. Under this approach, a designer

selects an appropriate basis function for their application, e.g., polynomial splines [13], [14], Bezier curves [15], Fourier transforms [16], or piece-wise constant functions [17]. The parameters of these basis functions are optimally determined before they are transformed back to the original coordinates of the nonlinear dynamical system, which yields the optimal trajectory for the selected basis. A rigorous overview of this approach is given in a recent textbook [18].

In contrast, our approach is classified as indirect as we seek a solution from the optimality conditions. There is similar results for the so-called maximal inversion approach [19], [20], which proves that the optimality conditions for a differentially flat system can be separated into two parts—one describing the optimal state trajectory, and the other describing the optimal costate trajectory. This result is significant, as the general optimality conditions couple the evolution of the states and costates, which can lead to significant numerical instabilities [21]. While the authors in [20] proved that the optimality conditions are separable, in this paper, we provide the analytical form of the ordinary differential equation that describes their evolution. Furthermore, the results in [20] consider control-affine nonlinear systems. In contrast, in our approach, we do not require affinity in the control. We also derive the optimal boundary conditions in the flat output space, which, to the best of our knowledge, has not been addressed in the literature to date. Finally, while recent work employs saturation functions to handle trajectory constraints [22], we analyze the state and control constraints directly. The main contributions of this paper are:

- 1) We present a set of ordinary differential equations that describe the evolution of the costates as explicit functions of the state and control variables (Theorem 1).
- 2) We derive an equivalent set of optimality conditions that are independent of the costates (Theorem 2). This independence property holds for interior-point constraints (Section III-B) and trajectory constraints (Section III-C).
- 3) We derive equivalent boundary conditions for the state and control variables when an initial or final state is left free or when the final time is unknown (Section III-D).
- 4) We demonstrate a significant improvement in computational time and total cost compared to general-purpose numerical solvers (Section IV).

The remainder of the manuscript is organized as follows. In Section II, we provide the modeling framework and enumerate our assumptions before presenting our main theoretical results in Section III. Then, in Section IV, we provide an illustrative example of controlling a double-integrator agent to avoid an obstacle and compare the performance of our approach to existing off-the-shelf optimal control libraries. Finally, we

This research was supported by the Sociotechnical Systems Center (SSC) at the University of Delaware.

L.E. Beaver and A.A. Malikopoulos are with the Department of Mechanical Engineering, University of Delaware, Newark, DE (emails: lebeaver@udel.edu, andreas@udel.edu).

draw concluding remarks and present directions of future work in Section V.

II. PROBLEM FORMULATION

Consider the nonlinear dynamical system,

$$\dot{\mathbf{x}}(t) = \mathbf{f}(\mathbf{x}(t), \mathbf{u}(t)), \quad (1)$$

where $\mathbf{x}(t) \in \mathbb{R}^n$ and $\mathbf{u}(t) \in \mathbb{R}^m$, $n < m$, are the state and control vectors, respectively, and $t \in \mathbb{R}_{\geq 0}$ is time. A system is *differentially flat* if it satisfies the following definition.

Definition 1 (Adapted from [23]). The system described by (1) is said to be differentially flat if there exists a vector $\mathbf{y}(t) = (y_1(t), \dots, y_m(t))$, such that:

- 1) The variables $y_i(t)$, $i = 1, \dots, m$ and their time derivatives are independent.
- 2) There exists a smooth mapping σ from $\mathbf{x}(t)$, $\mathbf{u}(t)$, and a finite number of its derivatives to \mathbf{y} , i.e.,

$$\mathbf{y}(t) = \sigma(\mathbf{x}(t), \mathbf{u}(t), \dot{\mathbf{u}}(t), \dots, \mathbf{u}^{(p)}(t)), \quad (2)$$

for some $p \in \mathbb{N}$.

- 3) The variables $\mathbf{x}(t)$ and $\mathbf{u}(t)$ can be expressed as smooth functions of $\mathbf{y}(t)$ and a finite number of its time derivatives, i.e.,

$$\mathbf{x}(t) = \gamma_0(\mathbf{y}(t), \dot{\mathbf{y}}(t), \dots, \mathbf{y}^{(q)}(t)), \quad (3)$$

$$\mathbf{u}(t) = \gamma_1(\mathbf{y}(t), \dot{\mathbf{y}}(t), \dots, \mathbf{y}^{(q)}(t)), \quad (4)$$

for some $q \in \mathbb{N}$.

Furthermore, σ , γ_0 , and γ_1 are smooth mappings between the flat and original spaces, thus, (2)–(4) constitute a diffeomorphism between the original and flat manifolds.

Note that the transformation between the original and output spaces achieved by (2) uses only the state and control variables, along with a finite number of derivatives. For this reason, differentially flat systems are also said to have *endogenous feedback*.

We impose the following assumptions for our analysis of the differentially flat system presented in Definition 1.

Assumption 1. The trajectory of the system is contained in open set where the functions (2)–(4) exist.

Assumption 2. The control actions in the original and flat spaces are upper and lower bounded.

Assumption 1 is a standard assumption in the literature [24] since there are no known algorithms that yield the mappings between the original and flat space [18]. Assumption 1 can be relaxed by constraining the trajectory to remain within a subset where (2)–(4) are defined.

Assumption 2 is standard in optimal control [25], particularly for physical systems where actuators are ultimately bounded by their physical strength or energy consumption. This assumption can be relaxed by allowing the control input to take the form of a Dirac delta function.

As an illustrative example of our approach, consider a unicycle traveling in the \mathbb{R}^2 plane.

Example 1. Let $\mathbf{x}(t) = [p_x(t), p_y(t), \theta(t)]^T$ be the state of a unicycle in the \mathbb{R}^2 plane, where $x(t)$ and $y(t)$ denote the position, and $\theta(t)$ denotes the heading angle. Let $\mathbf{u}(t) = [u_1(t), u_2(t)]^T$ be the vector of control actions, where $u_1(t)$ and $u_2(t)$ denote the forward and angular velocity, respectively. Then, the dynamics are given by

$$\dot{\mathbf{x}}(t) = \begin{bmatrix} u_1(t) \cos(\theta(t)) \\ u_1(t) \sin(\theta(t)) \\ u_2(t) \end{bmatrix}. \quad (5)$$

This system admits $m = 2$ differentially flat output variables, $\mathbf{y}(t) = [y_1(t), y_2(t)]^T = [p_x(t), p_y(t)]^T$ [18]. The transformations (3) and (4) between the flat outputs and original coordinates are

$$\begin{bmatrix} p_x(t) \\ p_y(t) \\ \theta(t) \end{bmatrix} = \begin{bmatrix} y_1(t) \\ y_2(t) \\ \arctan2(\dot{y}_2, \dot{y}_1) \end{bmatrix}, \quad (6)$$

$$\begin{bmatrix} u_1(t) \\ u_2(t) \end{bmatrix} = \begin{bmatrix} \sqrt{\dot{y}_1(t)^2 + \dot{y}_2(t)^2} \\ \frac{\dot{y}_2 \dot{y}_1 - \dot{y}_2 \dot{y}_1}{\dot{y}_2^2 + \dot{y}_1^2} \end{bmatrix}, \quad (7)$$

which obey Assumption 1 for $u_1(t) \neq 0$.

Finally, consider a constrained optimal control problem for a system governed by (1) under Assumptions 1 and 2.

Problem 1. Consider the differentially flat system with running cost $L(\mathbf{x}(t), \mathbf{u}(t))$ over the time horizon $[t^0, t^f] \subset \mathbb{R}_{\geq 0}$ and a final cost $\phi(\mathbf{x}(t^f), \mathbf{u}(t^f))$. Determine the optimal control input that minimizes the total cost, i.e.,

$$\min_{\mathbf{u}(t)} \phi(\mathbf{x}(t^f), \mathbf{u}(t^f)) + \int_{t^0}^{t^f} L(\mathbf{x}(t), \mathbf{u}(t)) dt$$

subject to: (1),

$$\hat{\mathbf{g}}(\mathbf{x}(t), \mathbf{u}(t), t) \leq 0,$$

given: initial conditions, final conditions,

where the initial and final states may be fixed, a function of the state variables, or left free. In addition, the function $\hat{\mathbf{g}}(\mathbf{x}(t), \mathbf{u}(t), t)$ defines a vector of state and control trajectory constraints.

In what follows, we present our main results, which yield a set of sufficient conditions for optimality that are only dependent on the state and control variables.

III. MAIN RESULTS

A. Separability of the Optimality Conditions

We can convert Problem 1 into Brunovsky normal form using the flat output variables $\mathbf{y}(t) \in \mathbb{R}^m$ [24]. This yields a set of integrator chains starting from $\mathbf{y}(t)$,

$$\begin{aligned} \dot{y}_i^{(j)}(t) &= y_i^{(j+1)}(t), & i &= 1, 2, \dots, m, \\ j &= 0, 1, \dots, k_i - 1, \end{aligned} \quad (8)$$

where $y_i^{(j)}(t)$ is the j th time derivative of base state $y_i(t)$ and $k_i \in \mathbb{N}$ is the length of the integrator chain for each base state. Next, we define equivalent state and control vectors for the system in the flat output space.

Definition 2. The dynamics of the system in the flat output space consists of m integrator chains of size k_i for $i = 1, 2, \dots, m$. The state vector $\mathbf{s}(t)$ and control vector $\mathbf{a}(t)$ are

$$\mathbf{s}(t) = \left[y_1(t), \dots, y_1^{(k_1-1)}(t), \dots, y_m^{(k_m-1)}(t) \right]^T, \quad (9)$$

$$\mathbf{a}(t) = \left[y_1^{(k_1)}(t), \dots, y_m^{(k_m)}(t) \right]^T. \quad (10)$$

Remark 1. For the unicycle system in Example 1, the flat state and control variables are

$$\mathbf{s}(t) = \left[y_1(t), y_2(t), \dot{y}_1(t), \dot{y}_2(t) \right]^T, \quad (11)$$

$$\mathbf{a}(t) = \left[\ddot{y}_1(t), \ddot{y}_2(t) \right]^T, \quad (12)$$

which consists of two integrator chains, each with a length of $k_i = 2$, for $i = 1, 2$.

Next, we apply (3) and (4) (Definition 1) to map Problem 1 to the flat output space.

Problem 2. Find the cost-minimizing trajectory in the flat output space,

$$\begin{aligned} \min_{\mathbf{a}(t)} \quad & \Phi(\mathbf{s}(t^f), \mathbf{a}(t^f)) + \int_{t^0}^{t^f} \Psi(\mathbf{s}(t), \mathbf{a}(t)) dt \\ \text{subject to:} \quad & (8), \\ & \mathbf{g}(\mathbf{s}(t), \mathbf{a}(t), t) \leq 0, \\ & \text{given: initial conditions, final conditions,} \end{aligned}$$

where Φ , Ψ , \mathbf{g} , and the boundary conditions are constructed by composing ϕ , L , $\hat{\mathbf{g}}$, and the original boundary conditions of Problem 1 with the inverse of (3) and (4). Without loss of generality, we consider that \mathbf{g} is an explicit function of at least one component of the control variable in the remainder of this section. We prove that this is eventually implied by Assumption 2 in Section III-C.

Note that Problem 2 takes the nonlinearities of the original system dynamics and moves them into the objective function and constraints. This can be advantageous for optimal control problems, where satisfying kinematic constraints can lead to significant numerical challenges.

Next, we present our first main result, which decouples the state and costates for the Hamiltonian function associated with Problem 2.

Theorem 1. The costates $\lambda^{y_i^{(j)}}$ for each base state $i = 1, 2, \dots, m$ and $j = 0, 1, \dots, k_i - 1$ that correspond to Problem 2 are equal to

$$\lambda^{y_i^{(j)}} = \sum_{n=1}^{k_i-j} (-1)^n \frac{d^{n-1}}{dt^{n-1}} \left(\Psi_{y_i^{(j+n)}} + \boldsymbol{\mu}^T \mathbf{g}_{y_i^{(j+n)}} \right). \quad (13)$$

Proof. We follow the standard process for solving optimal control problems [25], [26]. First, we construct the Hamiltonian for Problem 2,

$$\begin{aligned} H = \Psi(\mathbf{s}(t), \mathbf{a}(t)) + \boldsymbol{\lambda}^T(t) \mathbf{I}(\mathbf{s}(t), \mathbf{a}(t)) \\ + \boldsymbol{\mu}^T \mathbf{g}(\mathbf{x}(t), \mathbf{u}(t), t), \end{aligned} \quad (14)$$

where $\boldsymbol{\lambda}(t)$ is the vector of costates, $\mathbf{I}(\mathbf{s}(t), \mathbf{a}(t))$ corresponds to the integrator dynamics, defined by (8), \mathbf{g} is a vector of

inequality constraints, and $\boldsymbol{\mu}$ is a vector of inequality Lagrange multipliers. To simplify the notation, we omit the explicit dependence on $\mathbf{a}(t)$, $\mathbf{s}(t)$, and t where it does not lead to ambiguity. The Euler-Lagrange equations are

$$-\dot{\boldsymbol{\lambda}}^T = \Psi_{\mathbf{s}} + \boldsymbol{\lambda}^T \mathbf{I}_{\mathbf{s}} + \boldsymbol{\mu}^T \mathbf{g}_{\mathbf{s}}, \quad (15)$$

$$0 = \Psi_{\mathbf{a}} + \boldsymbol{\lambda}^T \mathbf{I}_{\mathbf{a}} + \boldsymbol{\mu}^T \mathbf{g}_{\mathbf{a}}, \quad (16)$$

where the subscripts \mathbf{a} and \mathbf{s} correspond to partial derivatives with respect to those variables. We simplify (15) by exploiting the integrator structure of \mathbf{I} for each element of $\mathbf{s}(t)$. This yields,

$$\dot{\lambda}^{y_i} = -\Psi_{y_i} - \boldsymbol{\mu}^T \mathbf{g}_{y_i}, \quad (17)$$

$$\dot{\lambda}^{y_i^{(j)}} = -\Psi_{y_i^{(j)}} - \lambda^{y_i^{(j-1)}} - \boldsymbol{\mu}^T \mathbf{g}_{y_i^{(j)}}, \quad (18)$$

for $i \in \{1, 2, \dots, m\}$ and $j \in \{1, 2, \dots, k_i - 1\}$. Similarly, simplifying each column of (16) yields

$$\lambda^{y_i^{(k_i-1)}} = -\Psi_{y_i^{(k_i)}} - \boldsymbol{\mu}^T \mathbf{g}_{y_i^{(k_i)}}, \quad (19)$$

for each output $i \in \{1, 2, \dots, m\}$. Note that (19) satisfies (13) for $j = k_i - 1$. Next, taking a time derivative of (19) and substituting it into (18) with $j = k_i - 1$ yields

$$\frac{d}{dt} \left(\Psi_{y_i^{(k_i)}} + \boldsymbol{\mu}^T \mathbf{g}_{y_i^{(k_i)}} \right) = \Psi_{y_i^{(k_i-1)}} + \boldsymbol{\mu}^T \mathbf{g}_{y_i^{(k_i-1)}} + \lambda^{y_i^{(k_i-2)}},$$

which implies,

$$\begin{aligned} \lambda^{y_i^{(k_i-2)}} = & - \left(\Psi_{y_i^{(k_i-1)}} + \boldsymbol{\mu}^T \mathbf{g}_{y_i^{(k_i-1)}} \right) \\ & + \frac{d}{dt} \left(\Psi_{y_i^{(k_i)}} + \boldsymbol{\mu}^T \mathbf{g}_{y_i^{(k_i)}} \right), \end{aligned} \quad (20)$$

which satisfies (13) for $j = k_i - 2$. Taking repeated time derivatives of (20) and substituting (18) completes the proof of Theorem 1. \square

Remark 2. For the unicycle system in Example 1, the covectors are

$$\boldsymbol{\lambda}^y = -(\psi_{\dot{y}} + \boldsymbol{\mu}^T \mathbf{g}_{\dot{y}}) + \frac{d}{dt} (\psi_{\mathbf{a}} + \boldsymbol{\mu}^T \mathbf{g}_{\mathbf{a}}), \quad (21)$$

$$\boldsymbol{\lambda}^{y^{(1)}} = -(\psi_{\mathbf{a}} + \boldsymbol{\mu}^T \mathbf{g}_{\mathbf{a}}). \quad (22)$$

Applying Theorem 1 to the Euler-Lagrange equations yields an equivalent set of optimality conditions that are independent of the costate variables, which we present in Theorem 2.

Theorem 2. The optimal trajectory for the system described in Problem 2 satisfies

$$\sum_{n=0}^{k_i} (-1)^n \frac{d^n}{dt^n} \left(\Psi_{y_i^{(n)}} + \boldsymbol{\mu}^T \mathbf{g}_{y_i^{(n)}} \right) = 0, \quad (23)$$

for each integrator chain starting with the base state y_i , $i = 1, 2, \dots, m$.

Proof. By Theorem 1,

$$\lambda^{y_i} = \sum_{n=1}^{k_i} (-1)^n \frac{d^{n-1}}{dt^{n-1}} \left(\Psi_{y_i^{(n)}} + \boldsymbol{\mu}^T \mathbf{g}_{y_i^{(n)}} \right). \quad (24)$$

Taking the derivative of (24) and substituting (17) yields,

$$\begin{aligned}\dot{\lambda}^{y_i} &= -\Psi_{y_i} - \boldsymbol{\mu}^T \mathbf{g}_{y_i} \\ &= \sum_{n=1}^{k_i} (-1)^n \frac{d^n}{dt^n} (\Psi_{y_i^{(n)}} + \boldsymbol{\mu}^T \mathbf{g}_{y_i^{(n)}}).\end{aligned}\quad (25)$$

This simplifies to

$$\Psi_{y_i} + \boldsymbol{\mu}^T \mathbf{g}_{y_i} + \sum_{n=1}^{k_i} (-1)^n \frac{d^n}{dt^n} (\Psi_{y_i^{(n)}} + \boldsymbol{\mu}^T \mathbf{g}_{y_i^{(n)}}) = 0, \quad (26)$$

which proves Theorem 2. \square

Note that while we prove Theorem 2 for the flat output space, the diffeomorphism (3) and (4) can be composed with (23) to generate an equivalent optimality condition in the original space. This implies that the state and costate dynamics can always be separated, and that this property is independent of the coordinate system.

Remark 3. Applying Theorem 2 to Example 1 yields the optimality equation,

$$(\Psi_p + \boldsymbol{\mu}^T \mathbf{g}_p) - \frac{d}{dt} (\Psi_v + \boldsymbol{\mu}^T \mathbf{g}_v) + \frac{d^2}{dt^2} (\Psi_a + \boldsymbol{\mu}^T \mathbf{g}_a) = 0.$$

Theorem 2 describes the evolution of the optimal state trajectory. When a constraint becomes active, i.e., strictly equal to zero, discontinuities may occur in the control action and the costates. Following the standard approach [25], these discontinuities must satisfy a set of optimality conditions,

$$\boldsymbol{\lambda}^{-T} = \boldsymbol{\lambda}^{+T} + \boldsymbol{\pi}^T \mathbf{N}_s, \quad (27)$$

$$H^+ - H^- = \boldsymbol{\pi}^T \mathbf{N}_t, \quad (28)$$

$$\frac{\partial H^-}{\partial \mathbf{a}^-} = \frac{\partial H^+}{\partial \mathbf{a}^+} = \mathbf{0}, \quad (29)$$

where the superscripts $-$ and $+$ denote the instant in time just before and just after the activation, respectively, $\boldsymbol{\pi}$ is a constant vector of Lagrange multipliers, \mathbf{N} is a vector of tangency conditions, which we rigorously derive in the following subsections, and the subscripts s and t correspond to partial derivatives with respect to the state and time.

Equivalently, we interpret Theorem 2 as generating optimal motion primitives for the system's trajectory. Let \mathbf{g} have c linearly independent rows, then $\boldsymbol{\mu}$ is a $c \times 1$ matrix. When a constraint g_i , $i = 1, 2, \dots, c$ does not influence the system trajectory, we can equivalently state that $\mu_i(t) = 0$. Therefore, we can generate 2^c motion primitives by setting combinations of elements in $\boldsymbol{\mu}$ equal to zero. In this context, the conditions (27)–(29) describe the optimal transition between different motion primitives along the system's trajectory. As an example, we present the optimality conditions for the unconstrained trajectory next.

Corollary 1. The evolution of the optimal unconstrained trajectory obeys

$$\sum_{j=0}^{k_i} (-1)^j \frac{d^j}{dt^j} \Psi_{y_i^{(j)}} = 0. \quad (30)$$

Proof. The result follows by substituting $\boldsymbol{\mu} = \mathbf{0}$ into (23). \square

In the following sections we analyze how the state trajectory is affected by the activation of state and control constraints during operation. Note that the transition between optimal motion primitives can be written independently of the costate dynamics by applying Theorem 1 to (27)–(29).

B. Interior-Point Constraints

First, we will consider the case where a set of state and/or control values are imposed at a single time instant. Let $\mathbf{h}(\mathbf{x}(t_1), t_1) = \mathbf{0}$ describe an interior point constraint that is imposed at some time t_1 . We construct the tangency vector,

$$\mathbf{N}(\mathbf{x}(t), t) = \begin{bmatrix} \mathbf{h}(\mathbf{x}(t), t) \\ t - t_1 \end{bmatrix}, \quad (31)$$

which guarantees constraint satisfaction when $\mathbf{N}(\mathbf{x}(t_1), t_1) = \mathbf{0}$. Note that if the time t_1 is unknown, then (31) is equal to \mathbf{h} . The tangency vector (31) is directly substituted into the optimality equations (27) and (28). Finally, applying Theorem 1 to (27)–(29) yields $\sum_{i=1}^m \{k_i - 1\} + 1$ equations that determine the optimal change in \mathbf{a} and its derivatives at t_1 . These equations are independent of the costate vectors. Further manipulating (27)–(29) yields a useful pair of equations that are amenable to finding an analytical solution. First, we substitute (14) into (28) and use (27) to eliminate $\boldsymbol{\lambda}^-$,

$$\begin{aligned}(\Psi^+ - \Psi^-) + (\boldsymbol{\mu}^{+T} \mathbf{g}^+ - \boldsymbol{\mu}^{-T} \mathbf{g}^-) \\ + \boldsymbol{\lambda}^{+T} (\mathbf{I}^+ - \mathbf{I}^-) = \boldsymbol{\pi}^T (\mathbf{N}_t + \mathbf{N}_s \mathbf{I}^-).\end{aligned}\quad (32)$$

Note that, by definition, $\boldsymbol{\mu}^T \mathbf{g} = 0$ along the optimal state-trajectory, thus we set those terms equal to zero. Furthermore, the state trajectory is continuous under Assumption 2 and the integrator dynamics. Thus,

$$\mathbf{I}^+ - \mathbf{I}^- = \begin{bmatrix} \mathbf{0} \\ \mathbf{a}^+ - \mathbf{a}^- \end{bmatrix}. \quad (33)$$

Applying Theorem 1 to (32) for the case $j = k_i - 1$ and simplifying yields,

$$\begin{aligned}(\Psi^+ - \Psi^-) - (\Psi_{\mathbf{a}} + \boldsymbol{\mu}^T \mathbf{g}_{\mathbf{a}})^- \cdot (\mathbf{a}^+ - \mathbf{a}^-) \\ = \boldsymbol{\pi}^T (\mathbf{N}_t + \mathbf{N}_s \mathbf{I}^+).\end{aligned}\quad (34)$$

Following a similar process also implies,

$$\begin{aligned}(\Psi^+ - \Psi^-) - (\Psi_{\mathbf{a}} + \boldsymbol{\mu}^T \mathbf{g}_{\mathbf{a}})^+ \cdot (\mathbf{a}^+ - \mathbf{a}^-) \\ = \boldsymbol{\pi}^T (\mathbf{N}_t + \mathbf{N}_s \mathbf{I}^-).\end{aligned}\quad (35)$$

C. Trajectory Constraints

Next, we consider the case where the state and/or control constraints imposed on Problem 2 influence the trajectory of the system. To generate our optimal motion primitive using Theorem 2, we first need to ensure our constraints are functions of the state and control variables. Let $h_i(\mathbf{s}(t), t) \leq 0$ denote the $i = 1, 2, \dots, c$ state or control constraints that are imposed on Problem 2. Note that h_i may not explicitly be a function of the control input. Under the standard approach [25], we require that h_i is at least q_i -times differentiable, where q_i is the minimum number of derivatives required for any component of the control input to appear in $\frac{d^{q_i}}{dt^{q_i}} h_i$.

To guarantee satisfaction of the original constraint h_i , we construct the tangency vector,

$$\mathbf{N}_i(\mathbf{s}(t), t) := \begin{bmatrix} h_i(\mathbf{s}(t), t) \\ h_i^{(1)}(\mathbf{s}(t), t) \\ \vdots \\ h_i^{(q_i-1)}(\mathbf{s}(t), t) \end{bmatrix}, \quad (36)$$

and we define the constraint

$$g_i(\mathbf{s}(t), \mathbf{a}(t), t) := h_i^{(q_i)}(\mathbf{s}(t), \mathbf{a}(t), t). \quad (37)$$

Thus, whenever $h_i(\mathbf{s}(t), t) = 0$ over a non-zero interval, we impose $\mathbf{N}_i(\mathbf{s}(t), t) = \mathbf{0}$ and $\mathbf{g}_i(\mathbf{s}(t), \mathbf{a}(t)) = 0$ over its interior to guarantee constraint satisfaction. This is equivalent to satisfying the original constraint under Assumption 2 [25]. Note that, if \mathbf{h}_i is explicitly a function of the control variable, $q = 0$ and \mathbf{N}_i is a zero-element vector. Furthermore, if the constraint is active over a zero-length interval, the problem reduces to the analysis in Section III-B with an unknown activation time.

Finally, to construct the tangency matrix for the c constraints, we construct the stacked tangency vector,

$$\mathbf{N}(\mathbf{s}(t), t) = \begin{bmatrix} \mathbf{N}_1(\mathbf{s}(t), t) \\ \mathbf{N}_2(\mathbf{s}(t), t) \\ \vdots \\ \mathbf{N}_c(\mathbf{s}(t), t) \end{bmatrix}, \quad (38)$$

which accounts for all of the constraints that may influence the state and control trajectory. As with the previous section, (27)–(29) determine the required instantaneous change in the control variables and their derivatives for an optimal trajectory. Note that, by construction,

$$\boldsymbol{\pi}^T \dot{\mathbf{N}}^+ = 0, \quad (39)$$

as $\mathbf{N}_i = \mathbf{0}$ and $\mathbf{g}_i^+ = 0$ when constraint i is active, and the corresponding $\boldsymbol{\pi}_i = 0$ otherwise. Thus, taking the full derivative implies,

$$\boldsymbol{\pi}^T \dot{\mathbf{N}}^+ = \boldsymbol{\pi}^T (\mathbf{N}_t + \mathbf{N}_s \cdot \mathbf{I}^+) = \mathbf{0}, \quad (40)$$

by construction. Thus, applying (34) at the end of a constrained motion primitive yields

$$(\Psi^+ - \Psi^-) - (\Psi_{\mathbf{a}} + \boldsymbol{\mu}^T \mathbf{g}_{\mathbf{a}})^- \cdot (\mathbf{a}^+ - \mathbf{a}^-) = 0. \quad (41)$$

This leads directly to our next result,

Corollary 2. If the system exits from or enters to an unconstrained motion primitive, the optimal control input satisfies

$$\Psi^+ - \Psi^- - \Psi_{\mathbf{a}}^-(a^+ - a^-) = 0, \quad \text{or} \quad (42)$$

$$\Psi^+ - \Psi^- - \Psi_{\mathbf{a}}^+(a^+ - a^-) = 0, \quad \text{respectively.} \quad (43)$$

Proof. When the system exits from an unconstrained motion primitive, $\boldsymbol{\mu}^- = \mathbf{0}$ and the result follows by (41). When the system enters an unconstrained motion primitive, $\boldsymbol{\mu}^+ = \mathbf{0}$ and $\boldsymbol{\pi} = \mathbf{0}$, thus the result follows by (34). \square

D. Boundary Conditions

The results of Sections III-B and III-C completely describe the evolution of the system if the boundary conditions are known. Next, we extend this result to the case that a boundary condition is unspecified by applying Theorem 1.

Corollary 3. Let the state $y_i^{(j)}(t)$ for $i \in \{1, 2, \dots, m\}$ and $j \in \{0, 1, 2, \dots, k_i - 1\}$ be unspecified at a boundary, i.e., it can be arbitrarily selected. There exists an equivalent boundary condition that guarantees optimality of the system trajectory.

Proof. Without loss of generality, let the state variable $y_i^{(j)}(t)$ be undefined at the final time t^f . Under the standard approach [25], the corresponding boundary condition $\lambda y_i^{(j)}(t^f) = 0$ is required to guarantee optimality. Thus, by Theorem 1,

$$\sum_{n=1}^{k_i-j} (-1)^n \frac{d^{n-1}}{dt^{n-1}} (\Psi_{y_i^{(j+n)}} + \boldsymbol{\mu}^T \mathbf{g}_{y_i^{(j+n)}}) \Big|_{t^f} = 0 \quad (44)$$

is an equivalent boundary condition. \square

In practice, it is likely that Problem 2 will have boundary conditions defined by functions of the state variables. This may arise from undefined state variables, as with Corollary 3, or from mapping known boundary conditions to the flat output space using Definition 1. Without loss of generality, let $\mathbf{B}(\mathbf{x}(t^f), t^f) = 0$ describe the functional constraints at t^f . This implies that [25]

$$\boldsymbol{\lambda}^T(t^f) = \left(\frac{\partial \Psi}{\partial \mathbf{s}} + \boldsymbol{\nu} \frac{\partial \mathbf{B}}{\partial \mathbf{s}} \right) \Big|_{t=t^f}, \quad (45)$$

$$\mathbf{B}(\mathbf{x}(t^f), t^f) = \mathbf{0}, \quad (46)$$

where $\boldsymbol{\nu}$ is a constant Lagrange multiplier that guarantees constraint satisfaction. Applying Theorem 1 to (45) results in a system of equations that guarantees constraint satisfaction at the boundaries. Thus, the flat system is guaranteed to have m initial and final conditions.

Finally, it's possible that the boundary conditions are described at an unknown terminal time. In this case, the optimal terminal time t^f satisfies [25]

$$\Omega = \left[\frac{\partial \Phi}{\partial t} + \boldsymbol{\nu} \frac{\partial \mathbf{B}}{\partial t} + \left(\frac{\partial \Phi}{\partial \mathbf{s}} + \boldsymbol{\nu}^T \frac{\partial \mathbf{B}}{\partial \mathbf{s}} \right) \mathbf{I} + \Psi \right]_{t=t^f} = 0. \quad (47)$$

Thus, Problem 2 always corresponds to a two-point boundary value problem with m initial conditions and m final conditions that are independent of the costates. Furthermore, (47) can be employed to determine an unknown terminal time using standard techniques [25]. Next, we present a numerical example for generating the trajectory of a double-integrator system in real time.

IV. DOUBLE-INTEGRATOR EXAMPLE

In this section we consider an agent moving in \mathbb{R}^2 with the states,

$$\mathbf{x}(t) = [\mathbf{p}^T(t), \mathbf{v}^T(t)]^T, \quad (48)$$

where $\mathbf{p}(t) \in \mathbb{R}^2$ is the agent's position, and $\mathbf{v} \in \mathbb{R}^2$ is the agent's velocity. We consider double-integrator dynamics,

$$\dot{\mathbf{x}}(t) = [\mathbf{v}(t)^T, \mathbf{u}(t)^T]^T, \quad (49)$$

where $\mathbf{u}(t) \in \mathbb{R}^2$ is the control action, which is bounded under Assumption 2. We consider the objective,

$$J(\mathbf{x}(t), \mathbf{u}(t)) = \frac{1}{2} \|\mathbf{u}(t)\|^2, \quad (50)$$

where the coefficient $\frac{1}{2}$ simplifies the derivative of J without influencing the optimal trajectory. This illustrative example is applicable to many mobile robots, including those with unicycle dynamics (Example 1) and differential drive robots.

First, we apply Theorem 1, which yields the costates,

$$\lambda^V(t) = -\mathbf{u}(t), \quad (51)$$

$$\lambda^P(t) = \dot{\mathbf{u}}(t). \quad (52)$$

Our objective is to move the system from a fixed initial state to a final position. If the initial and final states do not activate any constraints, the corresponding boundary conditions are

$$(\mathbf{p}(t^0), \mathbf{p}(t^f)) = (\mathbf{p}^0, \mathbf{p}^f), \quad (53)$$

$$(\mathbf{v}(t^0), \mathbf{u}(t^f)) = (\mathbf{v}^0, \mathbf{0}). \quad (54)$$

Note that the value of $\mathbf{u}(t^f)$ is implied by (51).

Let the agent be circumscribed in a circle of radius $R > 0$, and let the environment contains c obstacles that are indexed by the set $\mathcal{C} = \{1, 2, \dots, c\}$. Each obstacle $i \in \mathcal{C}$ is centered at the point $\mathbf{O}_i \in \mathbb{R}^2$ and has a radius $R_i \in \mathbb{R}_{>0}$. To guarantee safety, we impose the constraints

$$h_i(\mathbf{p}(t)) = D_i^2 - \hat{\mathbf{p}}_i(t) \cdot \hat{\mathbf{p}}_i(t) \leq 0, \quad (55)$$

where $D_i := R_i + R$ is the minimum separating distance between the agent and obstacle i and $\hat{\mathbf{p}}_i(t) := \mathbf{p}(t) - \mathbf{O}_i$. We use the equivalent squared form of (55) to simplify its time derivative. To simplify our analysis, we require obstacles to satisfy the spacing constraints,

$$\|\mathbf{O}_i - \mathbf{O}_j\| > D_i + D_j, \quad \forall i, j \in \mathcal{C}, i \neq j, \quad (56)$$

$$\|\mathbf{O}_i - \mathbf{p}^0\| > D_i \text{ and } \|\mathbf{O}_i - \mathbf{p}^f\| > D_i, \quad (57)$$

These spacing constraints are not restrictive on our approach, (56) ensures that only one obstacle avoidance constraint can become active at any instant in time, and (57) ensure that no constraints are active at the initial or final time. The constraints that we append to the Hamiltonian are the second derivative of (55),

$$\mathbf{g}_i(\mathbf{x}(t), \mathbf{u}(t)) := \mathbf{u}(t) \cdot \hat{\mathbf{p}}_i(t) + \mathbf{v}(t) \cdot \mathbf{v}(t) \leq 0. \quad (58)$$

Applying Theorem 2 in this context yields 2 motion primitives that completely describe the evolution of the system,

$$\text{unconstrained:} \quad \ddot{\mathbf{u}}(t) = \mathbf{0}, \quad (59)$$

$$\text{safety constrained:} \quad \ddot{\mathbf{u}}(t) + \ddot{\mu}(t)\hat{\mathbf{p}}_i(t) = \mathbf{0}. \quad (60)$$

Finally, we present Proposition 1, which describes the optimal transition between motion primitives.

Proposition 1. Continuity in the state variables, the $2m$ boundary conditions, the tangency conditions, and the following equations are sufficient to guarantee optimality when the system activates the safety constraint,

$$\mathbf{u}(t_1^-) = \mathbf{u}(t_1^+), \quad (61)$$

$$\mathbf{p}(t_1) \cdot \mathbf{v}(t_1) = 0, \quad (62)$$

$$\dot{\mathbf{u}}(t_1^-) \cdot \mathbf{v}(t_1) = \dot{\mathbf{u}}(t_1^+) \cdot \mathbf{v}(t_1), \quad (63)$$

The proof of Proposition 1 is presented in the Appendix. In the following subsections we derive the equations of motion for each of the motion primitives.

A. Optimal Motion Primitives

Under our imposed obstacle spacing (56), we must only consider two possible cases: no constraints influence the agent's trajectory, or avoiding one obstacle influences the agent's trajectory.

Case I: Unconstrained Motion. When the safety constraint is not active, the optimal control input is zero-snap, i.e., integrating (59) yields,

$$\mathbf{u}(t) = 6\mathbf{a}t + 2\mathbf{b}, \quad (64)$$

$$\mathbf{v}(t) = 3\mathbf{a}t^2 + 2\mathbf{b}t + \mathbf{c}, \quad (65)$$

$$\mathbf{p}(t) = \mathbf{a}t^3 + \mathbf{b}t^2 + \mathbf{c}t + \mathbf{d}, \quad (66)$$

where the constants of integration $\mathbf{a}, \mathbf{b}, \mathbf{c}, \mathbf{d}$ are determined by the boundary conditions. Thus, each unconstrained motion primitive introduces 8 unknowns.

Case II: Constrained Motion When the safety constraint is active, the tangency conditions imply that

$$\hat{\mathbf{p}}(t) \cdot \mathbf{v}(t) = 0. \quad (67)$$

Thus, taking the dot product of (60) with $\mathbf{v}(t)$ implies,

$$\ddot{\mathbf{u}}(t) \cdot \mathbf{v}(t) = 0. \quad (68)$$

Applying integration by parts to (68) yields,

$$\dot{\mathbf{u}}(t) \cdot \mathbf{v}(t) = C + \frac{1}{2} \mathbf{u}(t) \cdot \mathbf{u}(t), \quad (69)$$

where C is a constant of integration. Similarly, taking a derivative of (55) yields,

$$\dot{\mathbf{u}}(t) \cdot \mathbf{p}(t) = -3\mathbf{u}(t) \cdot \mathbf{v}(t). \quad (70)$$

Note that, by Proposition 1, each term in (69) and the right-hand side of (70) are both continuous. In addition, $\hat{\mathbf{p}}(t)$ and $\mathbf{v}(t)$ constitute an orthogonal basis for the system's trajectory. Thus, the constrained motion primitive is completely determined by the state of the system the instant it transitions, and it introduces only two unknowns—the entry and exit times.

Finally, for completeness, we must describe how the system transitions from the constrained motion primitive to the unconstrained motion primitive. In this case there are no active constraints, thus $\pi = \mathbf{0}$ in (27). Substituting (51) and (52) into (27) implies continuity in $\mathbf{u}(t)$ and $\dot{\mathbf{u}}(t)$, which, alongside continuity in the state, determines the unconstrained trajectory. Next, we solve these reduced systems of equations numerically and compare the performance to standard numerical solvers.

B. Numerical Simulation

To demonstrate the performance of our approach, we generated trajectories for the double integrator agent around a single obstacle. The parameters describing the simulation are presented in Table I, and the optimal trajectory is annotated in Fig. 1. For further details on our simulation approach, please see our public code repository on github¹.

\mathbf{p}^0 (m)	\mathbf{v}^0 (m/s)	\mathbf{p}^f (m)	\mathbf{O}_i (m)	D_i (m)	$t^f - t^0$ (s)
(-2, -2)	(0, 0)	(1, 2)	(0, 0)	1.25	10

TABLE I

BOUNDARY CONDITIONS AND OBSTACLE PARAMETERS THAT DESCRIBE THE SIMULATION ENVIRONMENT.

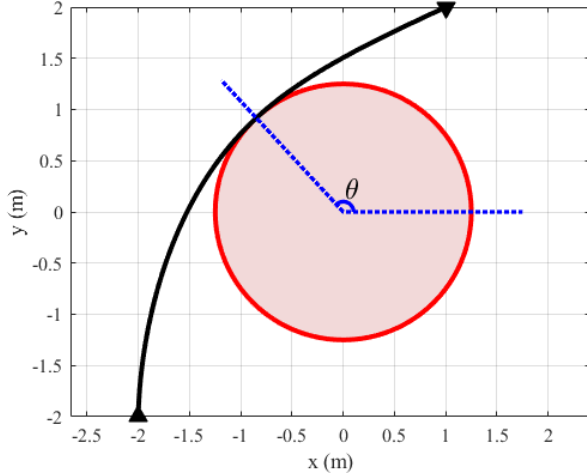


Fig. 1. Optimal trajectory (black) that avoids the obstacle (red). The variable θ describes where the trajectory instantaneously contacts the obstacle at time t_1 .

We apply the following steps to generate the optimal trajectory of the agent around the obstacle:

- 1) Connect the boundary conditions with an unconstrained motion primitive.
- 2) If the unconstrained trajectory is infeasible, find the optimal trajectory assuming the safety constraint is only activated instantaneously.
- 3) If the previous case is infeasible, find the optimal trajectory assuming the safety constraint is activated over a non-zero interval.

The first step consists of solving a set of 8 linear equations to determine the coefficients of the unconstrained motion primitive. This can be precomputed offline and has a negligible computational cost as a consequence. In the second step, we assume that the agent only contacts the obstacle instantaneously. The entire trajectory can be parameterized by two variables, (θ, t_1) ; Fig. 1 shows how θ defines the agent's trajectory relative to the obstacle. In the third step, we assume that the agent travels along the constrained motion primitive over a non-zero interval of time. The entire trajectory can be parameterized by three variables, (θ, t_1, t_2) .

After each step, we check if the resulting trajectory satisfies the collision avoidance constraint. If the initial unconstrained trajectory is infeasible, we use the time and angle of the constraint violation to calculate an initial guess for (θ, t_1) in Step 2. If the trajectory generated in Step 2 is infeasible, we reuse the values of θ and t_1 , as well as the earliest time that the constraint was violated, as an initial guess for (θ, t_1, t_2) . To demonstrate the performance of our approach, we generated

the optimal state trajectory for the agent in Matlab 2018b, using *fmincon* to solve the system of constrained nonlinear equations. We simulated the system on a desktop computer (Intel I5-3570k @3.4 GHz), and compared the performance to two general-purpose optimal control packages [27], [28]. We averaged the computation time over 10 trials; note that existing solvers use collocation methods, thus they require a large number of mesh points to guarantee constraint satisfaction near the obstacle. In contrast, our solution only saves the states at the boundary and motion primitives transitions. Table II demonstrates that our algorithm generates a superior trajectory in less time and with fewer mesh points stored in memory.

Approach	Time	Mesh Points	Cost	Max Violation
Proposed	34 ms	3	0.064 m/s ³	0 m
ICLOCS2	1500 ms	35	0.080 m/s ³	3×10^{-4} m
OpenCL	98 ms	35	0.080 m/s ³	4×10^{-15} m

TABLE II

PERFORMANCE COMPARISON OF THE GENERATED TRAJECTORIES.

V. CONCLUSION

In this paper, we proposed a technique to generate optimal trajectories for differentially flat systems. First, we derived an optimality condition that describes the optimal state evolution independently of the costates. Second, we applied Theorem 1 to derive additional boundary conditions for the flat system, which has not been presented in the literature to the best of our knowledge. Third, we proposed a motion primitive generator in Theorem 2 and derived the conditions to optimally switch between different motion primitives. Finally, we applied our results to a double-integrator system and generated a minimum-control trajectory with 20% less energy consumption and 2.8 times faster computational speed compared to existing solvers.

There are several intriguing directions for future work. First, it is practical, for given dynamics, to determine what functional forms of the objective guarantee that an analytical solution to (23) exists. Another potential direction for future research is to relax Assumptions 1 and 2 and derive similar results for systems with singularities and unbounded actuation capabilities. Finally, developing a general-purpose numerical method for differentially flat systems is another potential research direction.

ACKNOWLEDGEMENTS

We would like to thank Chris Kroninger and Michael Dorothy at DEVCOM Army Research Laboratory for their insightful discussions on optimal control.

APPENDIX 1

Proof of Proposition 1. There are two cases when system can transition between the constrained and unconstrained motion primitives.

Case I: Instantaneous Constraint Activation. In this case, the collision avoidance constraint is only activated instantaneously at some unknown time t_1 . Following the analysis in

¹<https://github.com/UD-IDS-LAB/Flatness-Obstacle-Avoidance>

Section III-B, and given the obstacle spacing constraint (56), we must only consider a single tangency equation,

$$\mathbf{N}(\mathbf{x}(t), t) = [D^2 - \hat{\mathbf{p}}_i(t) \cdot \hat{\mathbf{p}}_i(t)]. \quad (71)$$

The boundary conditions yield 8 equations, which can satisfy the 8 unknowns that describe one unconstrained motion primitive. When the safety constraint is activated instantaneously, the agent transitions between unconstrained motion primitives. This introduces 9 additional unknowns—the 8 coefficients of the new unconstrained motion primitive and the unknown transition time, t_1 . Proposition 1 provides the corresponding 9 equations: 4 from continuity in the state, 1 from (71), and 4 from (61)–(63). Condition (61) follows trivially from substituting (51) and (52) into (27), which yields,

$$\mathbf{u}^+ - \mathbf{u}^- = 0, \quad (72)$$

$$\dot{\mathbf{u}}^+ - \dot{\mathbf{u}}^- = 2\hat{\mathbf{p}}_i(t_1)\pi. \quad (73)$$

Furthermore, (35) implies that

$$0 = -2\pi\hat{\mathbf{p}}(t_1) \cdot \mathbf{v}(t_1). \quad (74)$$

This implies that either 1) $\pi = 0$ or 2) $\mathbf{p}(t_1) \cdot \mathbf{v}(t_1) = 0$. Assuming $\pi = 0$ implies that $\dot{\mathbf{u}}$ is continuous at t_1 , and thus both constrained motion primitives can be replaced with a single unconstrained motion primitive. This contradicts our premise that a constraint becomes active at t_1 . Therefore, the only possible solution is $\pi \neq 0$. This implies that $\mathbf{p}(t_1) \cdot \mathbf{v}(t_1) = 0$, which also implies (63) by taking dot product of (73) with $\mathbf{v}(t_1)$.

Case II: Transition to Constrained Motion Primitive.

In this case, the system transitions to a constrained motion primitive at t_1 , and it transitions back to another unconstrained motion primitive at some time $t_2 > t_1$. Following the analysis in Section III-C, we must satisfy,

$$\mathbf{N}(\mathbf{x}(t), t) = \begin{bmatrix} D_i^2 - \hat{\mathbf{p}}_i(t) \cdot \hat{\mathbf{p}}_i(t) \\ \mathbf{v}(t) \cdot \hat{\mathbf{p}}_i(t) \end{bmatrix} = \mathbf{0}, \quad (75)$$

$$\mathbf{g}(\mathbf{x}(t), \mathbf{u}(t)) = \mathbf{u}(t) \cdot \hat{\mathbf{p}}_i(t) + \mathbf{v}(t) \cdot \mathbf{v}(t) = 0, \quad (76)$$

over the open interval (t_1, t_2) . Thus, (62) is true via the tangency conditions. Corollary 2 implies,

$$\begin{aligned} & \|\mathbf{u}(t_1^+)\|^2 - \|\mathbf{u}(t_1^-)\|^2 - 2\mathbf{u}(t_1^-) \cdot (\mathbf{u}(t_1^+) - \mathbf{u}(t_1^-)) \\ &= \|\mathbf{u}(t_1^+)\|^2 + \|\mathbf{u}(t_1^-)\|^2 - 2\mathbf{u}(t_1^+) \cdot \mathbf{u}(t_1^-) = 0, \end{aligned} \quad (77)$$

which implies that $\mathbf{u}(t)$ is continuous at t_1 [29]. Finally, substituting (52) into (27) yields,

$$\dot{\mathbf{u}}(t_1^-) = \dot{\mathbf{u}}(t_1^+) + 2\hat{\mathbf{p}}(t_1)\pi_1\pi_2, \quad (78)$$

which implies (68) by dotting (78) with $\mathbf{v}(t_1)$. \square

REFERENCES

- [1] M. Rubenstein, C. Ahler, and R. Nagpal, “Kilobot: A low cost scalable robot system for collective behaviors,” in *Proceedings of the 2012 IEEE International Conference on Robotics and Automation*, 2012, pp. 3293–3298.
- [2] K. Jang, E. Vinitzky, B. Chalaki, B. Remer, L. Beaver, A. A. Malikopoulos, and A. Bayen, “Simulation to scaled city: zero-shot policy transfer for traffic control via autonomous vehicles,” in *Proceedings of the 10th ACM/IEEE International Conference on Cyber-Physical Systems*, 2019, pp. 291–300.
- [3] L. E. Beaver, B. Chalaki, A. M. Mahbub, L. Zhao, R. Zayas, and A. A. Malikopoulos, “Demonstration of a Time-Efficient Mobility System Using a Scaled Smart City,” *Vehicle System Dynamics*, vol. 58, no. 5, pp. 787–804, 2020.
- [4] B. Chalaki, L. E. Beaver, A. M. I. Mahbub, H. Bang, and A. A. Malikopoulos, “A scaled smart city for emerging mobility systems,” *arXiv:2109.05370*, 2021.
- [5] G. Vásárhelyi, C. Virágh, G. Somorjai, T. Nepusz, A. E. Eiben, and T. Vicsek, “Optimized flocking of autonomous drones in confined environments,” *Science Robotics*, vol. 3, no. 20, 2018.
- [6] A. M. I. Mahbub and A. Malikopoulos, “Concurrent optimization of vehicle dynamics and powertrain operation using connectivity and automation,” in *SAE Technical Paper 2020-01-0580*. SAE International, 2020).
- [7] A. A. Malikopoulos, L. E. Beaver, and I. V. Chremos, “Optimal time trajectory and coordination for connected and automated vehicles,” *Automatica*, vol. 125, no. 109469, 2021.
- [8] L. E. Beaver and A. A. Malikopoulos, “An Overview on Optimal Flocking,” *Annual Reviews in Control*, vol. 51, pp. 88–99, 2021.
- [9] H. Oh, A. R. Shirazi, C. Sun, and Y. Jin, “Bio-inspired self-organising multi-robot pattern formation: A review,” *Robotics and Autonomous Systems*, vol. 91, pp. 83–100, 2017.
- [10] M. Fliess, J. Lévine, P. Martin, and P. Rouchon, “Flatness and defect of non-linear systems: Introductory theory and examples,” *International Journal of Control*, vol. 61, no. 6, pp. 1327–1361, 1995.
- [11] N. Petit, M. B. Milam, and R. M. Murray, “Inversion Based Constrained Trajectory Optimization,” *IFAC Proceedings Volumes*, vol. 34, no. 6, pp. 1211–1216, 2001.
- [12] J. Lévine, “On The Equivalence Between Differential Flatness and Dynamic Feedback Linearizability,” *IFAC Proceedings Volumes*, vol. 40, no. 20, pp. 338–343, 2007.
- [13] D. Mellinger and V. Kumar, “Minimum snap trajectory generation and control for quadrotors,” in *IEEE International Conference on Robotics and Automation*, 2011, pp. 2520–2525.
- [14] K. Sreenath, N. Michael, and V. Kumar, “Trajectory generation and control of a quadrotor with a cable-suspended load - A differentially-flat hybrid system,” in *IEEE International Conference on Robotics and Automation*, 2013, pp. 4888–4895.
- [15] M. B. Milam, “Real-Time Optimal Trajectory Generation for Constrained Dynamical Systems,” Ph.D. dissertation, California Institute of Technology, 2003.
- [16] O. T. Ogunbodede, “Optimal Control of Differentially Flat Systems,” Ph.D. dissertation, The University at Buffalo, 2020.
- [17] B. Kolar, H. Rams, and K. Schlacher, “Time-optimal flatness based control of a gantry crane,” *Control Engineering Practice*, vol. 60, pp. 18–27, 3 2017.
- [18] H. Sira-Ramirez and S. K. Agrawal, *Differentially Flat Systems*, 1st ed. CRC Press, 2018.
- [19] F. Chaplais and N. Petit, “Inversion in indirect optimal control: constrained and unconstrained cases,” in *46th IEEE Conference on Decision and Control*, 2007, pp. 683–689.
- [20] —, “Inversion in indirect optimal control of multivariable systems,” *ESAIM: COCV*, vol. 14, pp. 294–317, 2008.
- [21] A. E. Bryson, “Optimal Control-1950 to 1985,” *IEEE Control Systems Magazine*, vol. 16, no. 3, pp. 26–33, 1996.
- [22] K. Graichen, A. Kugi, N. Petit, and F. Chaplais, “Handling constraints in optimal control with saturation functions and system extension,” *Systems and Control Letters*, vol. 59, no. 11, pp. 671–679, 11 2010.
- [23] J. Lévine, “On necessary and sufficient conditions for differential flatness,” *Applicable Algebra in Engineering, Communications and Computing*, vol. 22, no. 1, pp. 47–90, 2011.
- [24] M. Van Nieuwstadt, M. Rathinam, and R. M. Murray, “Differential flatness and absolute equivalence,” in *Proceedings of the IEEE Conference on Decision and Control*, vol. 1. IEEE, 1994, pp. 326–332.
- [25] A. E. J. Bryson and Y.-C. Ho, *Applied Optimal Control: Optimization, Estimation, and Control*. John Wiley and Sons, 1975.
- [26] I. M. Ross, *A Primer on Pontryagin’s Principle in Optimal Control*, 2nd ed., E. Solon, Ed. San Francisco: Collegiate Publishers, 2015.
- [27] Y. Nie, O. Faqir, and E. C. Kerrigan, “ICLOCS2: Try this Optimal Control Problem Solver Before you Try the Rest;” in *2018 UKACC 12th International Conference on Control (CONTROL)*, 2018.
- [28] J. Koenemann, G. Licitra, M. A. Politecnico, D. Milano, and M. Diehl, “OpenOCL - Open Optimal Control Library,” Tech. Rep., 2019.
- [29] L. E. Beaver, M. Dorothy, C. Kroninger, and A. A. Malikopoulos, “Energy-Optimal Motion Planning for Agents: Barycentric Motion and Collision Avoidance Constraints,” in *2021 American Control Conference*, 2021, pp. 1037–1042.